

Photoinduced spin-order destructions in one-dimensional extended Hubbard model

Hantao Lu¹, Shigetoshi Sota², Hiroaki Matsueda³, Janez Bonča^{4,5}, and Takami Tohyama¹

¹ Yukawa Institute for Theoretical Physics, Kyoto University, Kyoto, 606-8502, Japan

² Computational Materials Science Research Team, RIKEN AICS, Kobe, Hyogo 650-0047, Japan

³ Sendai National College of Technology, Sendai, 989-3128, Japan

⁴ Faculty of Mathematics and Physics, University of Ljubljana, SI-1000 Ljubljana, Slovenia

⁵ J. Stefan Institute, SI-1000 Ljubljana, Slovenia

E-mail: luht@yukawa.kyoto-u.ac.jp

Abstract. By employing the time-dependent Lanczos method, the nonequilibrium process of the half-filled one-dimensional extended Hubbard model under the irradiation of a transient laser pulse is investigated. We show that in the spin-density-wave (SDW) phase, the antiferromagnetic spin correlations are impaired by the photoinduced charge carriers. Near the phase boundary between the SDW and charge-density-wave (CDW) phases, a local enhancement of charge (spin) order that is absent in the original SDW (CDW) phase can be realized with proper laser frequency and strength. The possibility of restoration of spin orders from the CDW phase by optical means is discussed.

1. Introduction

New insights into the dynamics of strongly correlated electron systems can be achieved by investigating their nonequilibrium processes, which demands the knowledge and understanding of the properties of excited states. The process have to be treated nonperturbatively if the system is driven far from the equilibrium.

In experiments, one way to achieve nonequilibrium states is by applying various external electric fields, including pulses of electromagnetic field, which couple with charge degrees of freedom of the system. Well-known experimental facts on (quasi) one-dimensional (1D) materials include dielectric breakdown [1, 2], insulator to metal transitions and so on [3, 4, 5].

In Mott insulators, we have to deal with the states above the Mott gap in order to induce charge carriers optically. It is well known that the ground states of Mott insulators have quasi-long-range antiferromagnetic spin orders. The charge carriers created by photons are, thus, expected to affect the spin correlations. It is desirable to obtain the knowledge of spin dynamics, as well as the charge's, during and after the doping. In many 1D materials, it has been shown that besides the on-site Coulomb interaction U , nearest-neighbor (NN) interaction V has to be taken into account [6, 7]. With increase of V , a phase transition from the Mott insulator to a charge-order phase can occur. The nonequilibrium dynamics near the phase boundary is also important.

In this proceeding, we investigate the nonequilibrium process of a 1D strongly correlated system under the irradiation of a laser pulse. The model we are working on is the half-filled extended Hubbard model, where the on-site, and NN interactions (U and V), are included. Its phase diagram in equilibrium is well-known and understood [8, 9, 10, 11]. Here we would like to reiterate some known properties of the model, concerning our work. In strong-coupling regime (large $U(> 0)$), with increase of $V(> 0)$, a first-order phase transition from the spin-density-wave (SDW) to charge-density-wave (CDW) phase is realized when V reaches around $U/2$. The transition can be understood as driven by the competition between the energetic costs for doublon generation and the benefits due to the attraction between doublons and holons. The SDW and CDW phases are recognized by algebraic decay of spin correlations, and a long-range (staggered) charge order, respectively. In both phases, the charge sector is always gapped except on the boundary. When spin degrees of freedom are concerned, gapless spin modes can be found in the SDW phase, while absent in the CDW phase.

In the following sections, by studying time-dependent spin and charge correlation functions numerically, we show that spin correlations are suppressed by the photoinduced charge carriers in the SDW phase. Near the phase boundary from the SDW side, with proper laser frequency and strength, a sustainable charge order enhancement can be realized [12] but local spin correlations remains. Analogously, from the CDW side, the suppression of long-range charge order is accompanied with a local spin correlation enhancement.

2. Model and Numerical Method

The time-dependent Hamiltonian for the 1D extended Hubbard model, where the external field is incorporated by means of the Peierls substitution for the hopping coefficients, can be written as

$$\begin{aligned}
H(t) = & -t_h \sum_{i,\sigma} \left(e^{iA(t)} c_{i,\sigma}^\dagger c_{i+1,\sigma} + \text{H.c.} \right) \\
& + U \sum_i \left(n_{i,\uparrow} - \frac{1}{2} \right) \left(n_{i,\downarrow} - \frac{1}{2} \right) + V \sum_i (n_i - 1) (n_{i+1} - 1), \quad (1)
\end{aligned}$$

where $c_{i,\sigma}^\dagger$ ($c_{i,\sigma}$) creates (annihilates) electrons with spin σ at site i , $n_{i,\sigma} = c_{i,\sigma}^\dagger c_{i,\sigma}$, $n_i = n_{i,\uparrow} + n_{i,\downarrow}$, t_h is the hopping constant. Particularly, with temporal gauge, we use a time-dependent vector potential $A(t)$ to describe the laser pulse [13]

$$A(t) = A_0 e^{-(t-t_0)^2/2t_d^2} \cos[\omega_{\text{pump}}(t-t_0)], \quad (2)$$

where A_0 controls the laser amplitude, which reaches its full strength at $t = t_0$; t_d characterizes the duration time of light action. Note that, due to finite t_d , the incoming photon frequency is broadened into a Gaussian-like distribution, with the variance of $1/t_d^2$ around the central value ω_{pump} . Throughout this paper, we set t_h and t_h^{-1} as energy and time units.

Starting from the Schrödinger equation $i\partial\psi(t)/\partial t = H(t)\psi(t)$, in order to obtain $\psi(t)$, we employ the time-dependent Lanczos method, which is originally described in Ref. [14], and followed by its applications in nonequilibrium dynamics of strongly correlated systems recently in Ref. [15]. The basic idea is that we approximate the time evolution of $|\psi(t)\rangle$ by a step-wise change of time t in small increments δt . At each step, the Lanczos basis with dimension M is generated resulting in the time evolution

$$|\psi(t + \delta t)\rangle \simeq e^{-iH(t)\delta t} |\psi(t)\rangle \simeq \sum_{l=1}^M e^{-i\epsilon_l \delta t} |\phi_l\rangle \langle \phi_l | \psi(t)\rangle, \quad (3)$$

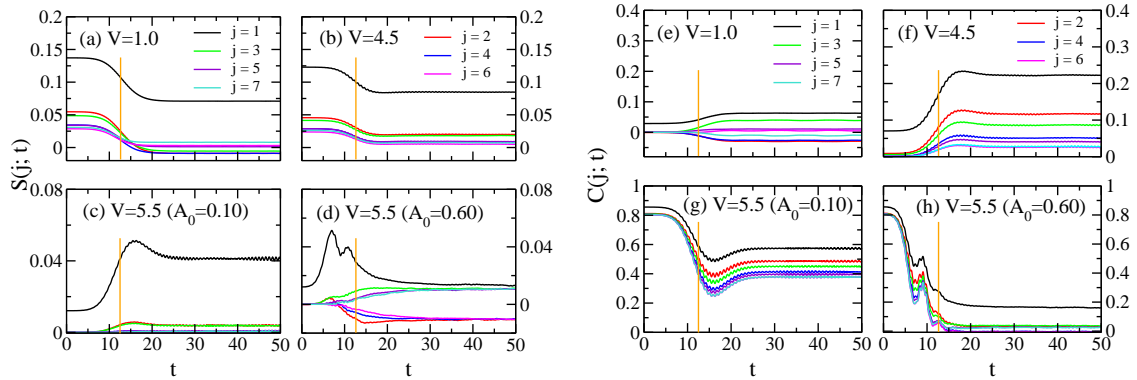


Figure 1. Time dependence of the spin-spin (left, from (a) to (d)) and charge-charge (right, from (e) to (h)) correlations as functions of distance (labeled by j) for 14-site lattice. The laser pulse with Gaussian magnitude modulation reaches its full strength at $t = 12.5$, as indicated by solid lines. Without exception, the pumping frequencies are set to match the resonance peaks of the optical absorption spectra. Parameters: $\delta t = 0.02$, $M = 100$. In each subfigure, (a),(e): $V = 1.0$, $\omega_{\text{pump}} = 7.1$, $A_0 = 0.10$; (b),(f): $V = 4.5$, $\omega_{\text{pump}} = 4.0$, $A_0 = 0.07$; (c),(g): $V = 5.5$, $\omega_{\text{pump}} = 4.1$, $A_0 = 0.10$; (d),(h): the same as (c) (or (g)), except for $A_0 = 0.60$.

where ϵ_l and $|\phi_l\rangle$, respectively, are eigenvalues and eigenvectors of the tridiagonal matrix generated in Lanczos iteration. As one of the advantages, the Lanczos method preserves the unitarity of the time-evolution operator at each time step, with relative low cost for a desired accuracy. The convergence check shows that for time length t around hundred, taking $M = 30$ with $\delta t \lesssim 0.1$ can provide adequate accuracy for the parameter regime we are working in. For even smaller δt , M can be smaller.

In the succeeding numerical calculations, periodic boundary conditions are employed to avoid possible boundary effects. We fix the parameters $t_d = 5$, $t_0 = 12.5$, and chose $U = 10$, where the first-order transition occurs around $V \approx 5.1$ [11].

3. Numerical Results

In order to investigate the time evolutions of the spin and charge orders under the pulses, we define the spin-spin and charge-charge correlations, respectively:

$$S(j;t) = \frac{(-1)^j}{L} \sum_{i=0}^{L-1} \langle \psi(t) | \mathbf{S}_{i+j} \cdot \mathbf{S}_i | \psi(t) \rangle, \quad (4a)$$

$$C(j;t) = \frac{(-1)^j}{L} \sum_{i=0}^{L-1} \langle \psi(t) | (n_{i+j} - 1)(n_i - 1) | \psi(t) \rangle, \quad (4b)$$

where L is the lattice size, and \mathbf{S}_i is the spin operator on site i . Intuitively, the antiferromagnetic spin and staggered charge orders are competitive.

Figure 1 shows the results of correlations $S(j;t)$, $C(j;t)$, up to $t = 50$, for the system with 14 lattice sites, where the largest distance between two sites is 7. Total crystal momentum P , as a good quantum number, is implemented. The size of the Hilbert space for $P = 0$ is 841332. For 2600 time step, it took around 30 hours for 12 cores. In succeeding discussions, we put more emphasis on spin. Detailed discussions on the charge correlations can be found in Ref. [12].

In Fig. 1, four cases are shown: (a) and (e), deep into the SDW phase ($V = 1$); (b) and (f), the ground state is near the phase boundary, but set on the SDW side ($V = 4.5$); (c) and (g),

(d) and (h), at the CDW side ($V = 5.5$) with different laser strength. Several observations can be made. First, notice that for the ground states (corresponding to $t = 0$) in the SDW phase, we can observe the gradually decay of spin correlations (Figs. 1(a), (b)) while no long-range charge order exists (Figs. 1(e), (f)); in the CDW phase, the presence of a long-range charge order can be clearly recognized (Figs. 1(g) or (h)), and the spin correlations largely vanish except for the NN one (See Figs. 1(c) or (d), where $S(j;0) \lesssim 10^{-4}$ for $j > 1$, and $S(1;0) \sim 0.01$). Second, for the case of $V = 1.0$, where the system is deep inside the SDW phase, introducing charge carriers into the system by the pulse cannot produce charge order (Fig. 1(e)), while the spin correlations are severely suppressed except for the NN one (See Fig. 1(a), where $S(1;t)$ decreases from 0.14 at $t = 0$ to 0.07 at $t = 50$, while some correlations with other distances even become negative). Notice that in this case, after the pulse, the total number of doublons (defined as $N_{\text{db}} = \sum_i n_{i,\uparrow} n_{i,\downarrow}$) is around 2.2, corresponding to 30% doping [16]. Third, we would like to pick up Fig. 1(f), which shows that proper incoming laser pulse can enhance the charge order considerably in the SDW near the phase boundary, where we can observe that the NN correlation increases from 0.07 at $t = 0$ to 0.22 at $t = 50$, together with a clear enhancement of other correlations in larger distances, which start from almost zero magnitudes at $t = 0$; meanwhile, the spin order does not suffer heavy suppression (See Fig. 1(b), where the NN correlation drops from 0.12 to 0.08). Analogously, from the CDW side close to the boundary, the pulse can suppress the charge order (Fig. 1(g)) with local spin enhancement taking place at the same time (Fig. 1(c), where the NN correlation increases from 0.01 to 0.04). Finally, from Fig. 1(d) and (h), we show that strong enough laser pulse can destroy the charge order substantially without spin correlation enhancement.

The results of the time-dependent correlations suggest intimate connections between spin and charge degrees of freedom in the photoexcited states. Interesting phenomena occur around the phase boundary, where local spin and charge orders can coexist. For a more quantitative analysis, we compare the spectra of systems with different values of V in the time-independent Hamiltonian, i.e., Eq. (1) but $A(t) = 0$. In order to describe the spin and charge orders which have finite spatial extensions, we define

$$\mathcal{O}_{\text{SDW}} = \frac{1}{LL_c} \sum_{i=0}^{L-1} \sum_{j=1}^{L_c} (-1)^j \mathbf{S}_{i+j} \cdot \mathbf{S}_i \quad (5a)$$

$$\mathcal{O}_{\text{CDW}} = \frac{1}{LL_c} \sum_{i=0}^{L-1} \sum_{j=1}^{L_c} (-1)^j (n_{i+j} - 1) (n_i - 1). \quad (5b)$$

Here L_c is introduced as a cut off parameter for the correlation length, and we set $L_c = 5$, estimated from the results of the density-matrix renormalization group (DMRG) on larger system size up to 30. The expectation values of the order parameter $\langle \mathcal{O}_{\text{CDW}} \rangle$ and $\langle \mathcal{O}_{\text{SDW}} \rangle$ for eigenstates of a smaller 10-site system are shown in Fig. 2.

In Fig. 2 from (a) to (d), we can notice that for $V = 1.0$ to 5.5, states with relative large $\langle \mathcal{O}_{\text{SDW}} \rangle$ are always situated in the low-energy regime (say, $E < 10$). On the contrary, states with prominent $\langle \mathcal{O}_{\text{CDW}} \rangle$ only appear there when the system is approaching the phase boundary. In Fig. 2(g) for $V = 4.5$, around the resonance frequency of optical absorption spectrum ($\omega_R \approx 4.3$), states with noticeable values of charge order can be found. This explains why a considerable charge order enhancement can be observed when the frequency of laser with proper strength is tuned to ω_R (see Fig. 1(f), where $\omega_R \approx 4.0$ for 14-site lattice). However, in the complementary case, only the enhancement of the NN spin correlation is apparently visible, with rapid decrease with increase of distance. The same holds for $L = 10$, in spite of the fact that a state with excitation energy $E \approx 2.7$ has a distinguished $\langle \mathcal{O}_{\text{SDW}} \rangle$ (shown by star in Fig. 2(d)).

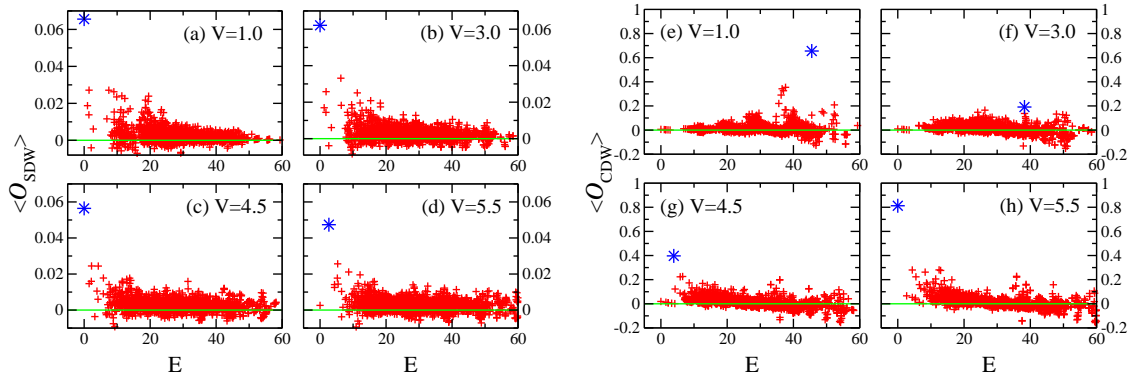


Figure 2. The expectations of SDW (from (a) to (d)) and CDW (from (e) to (h)) order parameters of eigenstates for 10-site lattice with $V = 1.0, 3.0, 4.5,$ and 5.5 . The energy E is measured from the ground state. Only the data of states with $P_{\text{tot}} = S_{\text{tot}} = 0$ are shown, up to $E = 60$. Note that the largest values of the order parameters in (a) through (h) are marked by stars.

In order to understand the different behavior of spin and charge correlations, and to further elaborate on the condition for the emergence of order enhancements induced by the laser pulse, we perform parameter-sweeping calculations in terms of ω_{pump} and A_0 for 10-site lattice. For a given pair of ω_{pump} and A_0 , we carry out the time evolutions up to $t = 52.5$, then calculate the expectations of the SDW order, CDW order, and doublon number, noted as $\langle \mathcal{O}_{\text{SDW}} \rangle_{\text{av}}$, $\langle \mathcal{O}_{\text{CDW}} \rangle_{\text{av}}$, and $\langle n_{\text{db}} \rangle_{\text{av}}$, respectively, after averaging on the last 50 time steps (corresponding to time length $\Delta t = 5$). The results, presented in contour plots, are shown in Fig. 3.

In Fig. 3, we notice that for each V , there exist some frequencies with which the optical absorptions are most efficient, e.g., $\omega_{\text{pump}} \approx 7.5$ in Fig. 3(i) for $V = 1.0$, $\omega_{\text{pump}} \approx 6.3$ in Fig. 3(j) for $V = 3.0$. These are resonance frequencies of optical absorption spectra ω_R , which can be obtained from the imaginary parts of the dynamical current-current correlation functions.

We can see that in order to excite the system effectively with weak fields, we need to tune the pulse frequency ω_{pump} close to ω_R . In general, in the SDW phase, accompanied with photodoping, spin correlations are suppressed (see the correspondence between the bright regions in Figs. 3(i), (j), (k) for doublon generation, and the dark regions in Figs. 3(a), (b), (c) for $\langle \mathcal{O}_{\text{SDW}} \rangle_{\text{av}}$). On the other hand, in the CDW phase, the destruction of charge order alone does not sufficiently bring back the spin order (see Fig. 3(l), compared with (d)).

Things can be more subtle near the phase boundary. With A_0 less than 0.1, a local enhancement of CDW order in the SDW phase can be induced accompanied with a suppression of spin orders, and vice versa in the CDW phase near the boundary. For example, see around $\omega_{\text{pump}} \approx 4.3$ in Figs. 3(g) and (c) for the case of $V = 4.5$, and $\omega_{\text{pump}} \approx 4.4$ in Figs. 3(d) and (h) for the case of $V = 5.5$. Among them, the weakness of the SDW enhancement in Fig. 3(d) can be attributed to the fact that the states with distinguished $\langle \mathcal{O}_{\text{SDW}} \rangle$ (around $E \approx 2.7$, see Fig. 2(d)) are in the off-resonance region, which makes it hard for them to be excited by the laser.

Going to the high-field region, we observe that in Fig. 3(d), at $\omega_{\text{pump}} \approx 1.2$, there is a well resolved stripe when $A_0 > 0.4$, indicating an enhancement of the spin order. From the results of $S(j; t)$ (not shown here), we notice that the spin correlations there extend themselves beyond NN. This may come from nonlinear multiphoton optical process [17]. Similar phenomenon for the case of charge order, can be found in Fig. 3(g), at $\omega_{\text{pump}} \approx 2$. Further investigation on the nonlinear effect is in progress.

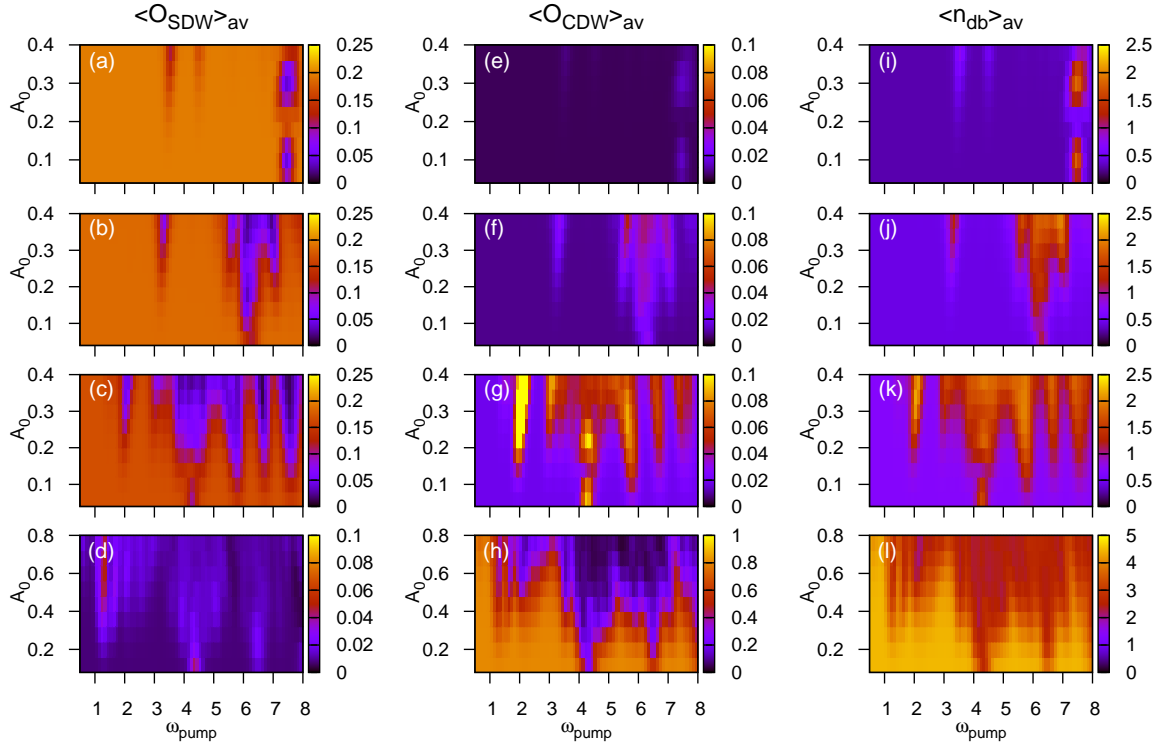


Figure 3. Contour plots of final time-evolution results of SDW order $\langle \mathcal{O}_{\text{SDW}} \rangle_{\text{av}}$ (first column), CDW order $\langle \mathcal{O}_{\text{CDW}} \rangle_{\text{av}}$ (second column) and doublon number N_{db} (last column) as functions of ω_{pump} and A_0 , obtained by averaging on the last 50 time steps (time length $\Delta t = 5$), for 10-site lattice. $\omega_{\text{pump}} \in [0.5, 8]$; $A_0 \in [0.04, 0.4]$ for the first three rows, and $[0.08, 0.8]$ for the last row. From top to bottom, $V = 1.0, 3.0, 4.5$, and 5.5 , respectively. Here, we take $\delta t = 0.1$, $M = 30$.

4. Conclusions

In summary, by studying time-dependent spin and charge correlation functions of the 1D extended Hubbard model with applied laser pulse, we have shown that in the SDW phase, the spin order is suppressed due to the optical doping. Starting from the SDW side not far from the phase boundary, when the incoming laser frequency matches the optical absorption peak, a sustainable charge order enhancement can be realized. Similarly, starting from the CDW side, an enhancement of spin correlations, though more localized, has been observed. In the off-resonance region, we find more extended recovery of spin correlations which may come from nonlinear effects.

References

- [1] Tokura Y, Okamoto H, Koda T, Mitani T and Saito G 1988 *Phys. Rev. B* **38**(3) 2215–2218 URL <http://link.aps.org/doi/10.1103/PhysRevB.38.2215>
- [2] Taguchi Y, Matsumoto T and Tokura Y 2000 *Phys. Rev. B* **62**(11) 7015–7018 URL <http://link.aps.org/doi/10.1103/PhysRevB.62.7015>
- [3] Iwai S, Ono M, Maeda A, Matsuzaki H, Kishida H, Okamoto H and Tokura Y 2003 *Phys. Rev. Lett.* **91**(5) 057401 URL <http://link.aps.org/doi/10.1103/PhysRevLett.91.057401>
- [4] Okamoto H, Matsuzaki H, Wakabayashi T, Takahashi Y and Hasegawa T 2007 *Phys. Rev. Lett.* **98** 037401 URL <http://link.aps.org/doi/10.1103/PhysRevLett.98.037401>
- [5] Kimura K, Matsuzaki H, Takaishi S, Yamashita M and Okamoto H 2009 *Phys. Rev. B* **79** 075116 URL <http://link.aps.org/doi/10.1103/PhysRevB.79.075116>

- [6] Yamashita M, Manabe T, Kawashima T, Okamoto H and Kitagawa H 1999 *Coord. Chem. Rev.* **190-192** 309–330 URL <http://linkinghub.elsevier.com/retrieve/pii/S0010854599000739>
- [7] Kumar M, Topham B J, Yu R, Ha Q B D and Soos Z G 2011 *J. Chem. Phys.* **134** 234304 (pages 8) URL <http://link.aip.org/link/?JCP/134/234304/1>
- [8] van Dongen P 1994 *Phys. Rev. B* **49** 7904–7915 URL <http://link.aps.org/doi/10.1103/PhysRevB.49.7904>
- [9] Nakamura M 2000 *Phys. Rev. B* **61** 16377–16392 URL <http://link.aps.org/doi/10.1103/PhysRevB.61.16377>
- [10] Tsuchiizu M and Furusaki A 2002 *Phys. Rev. Lett.* **88** 056402 URL <http://link.aps.org/doi/10.1103/PhysRevLett.88.056402>
- [11] Ejima S and Nishimoto S 2007 *Phys. Rev. Lett.* **99** 216403 URL <http://link.aps.org/doi/10.1103/PhysRevLett.99.216403>
- [12] Lu H, Sota S, Matsueda H, Bonča J and Tohyama T 2012 *Phys. Rev. Lett.* **109**(19) 197401 URL <http://link.aps.org/doi/10.1103/PhysRevLett.109.197401>
- [13] Matsueda H, Sota S, Tohyama T and Maekawa S 2012 *J. Phys. Soc. Jpn.* **81** 013701 URL <http://jpsj.ipap.jp/link?JPSJ/81/013701/>
- [14] Park T J and Light J C 1986 *J. Chem. Phys.* **85** 5870–5876 URL <http://link.aip.org/link/doi/10.1063/1.451548>
- [15] Prelovšek P and Bonča J 2011 Ground State and Finite Temperature Lanczos Methods (*Preprint arXiv:1111.5931*) URL <http://arxiv.org/abs/1111.5931>
- [16] Takahashi A, Itoh H and Aihara M 2008 *Phys. Rev. B* **77** 205105 URL <http://link.aps.org/doi/10.1103/PhysRevB.77.205105>
- [17] Oka T 2012 *Phys. Rev. B* **86** 075148 URL <http://prb.aps.org/abstract/PRB/v86/i7/e075148>